Westinghouse Proprietary Class 3

WCAP-10108
REV. 1

CONDOR

A THERMAL-HYDRAULIC PERFORMANCE CODE FOR BOILING WATER REACTORS

C. A. Olson

December 1983

Approved: P. K. Doshi
P. K. Doshi, Manager
BWR Fuel Engineering

Approved: D. R. McClintock
D. R. McClintock, Manager
BWR Fuel

Approved: JKupo for FWK
F. W. Kramer, Manager
NFD Engineering

WESTINGHOUSE ELECTRIC CORPORATION
Nuclear Fuel Division
P. O. Box 3912
Pittsburgh, Pennsylvania 15230

2120F:6/831209

TABLE OF CONTENTS

Section	Title	Page
	ACKNOWLEDGEMENTS	iv
	ABSTRACT	v
1.	INTRODUCTION	1-1
2.	GENERAL DESCRIPTION OF CONDOR CODE	2-1
	2.1 Purpose	2-1
	2.2 Brief Description of Core Analysis	2-1
3.	CONDOR METHODOLOGY	3-1
	3.1 Introduction	3-1
	3.2 Conservation Equations	3-1
	3.3 Void Models	3-4
	3.4 Bypass Flow Models	3-4
	3.5 Solution Technique	3-5
4.	VOID MODELS	4-1
	4.1 Levy's Model (Detached Voidage)	4-2
	4.2 Bulk Boiling	4-4
5.	PRESSURE DROP CORRELATION	5-1
	5.1 Introduction	5-1
	5.2 Single Phase Friction	5-1
	5.3 Two Phase Friction	5-1
	5.4 Single Phase Form	5-2
	5.5 Two Phase Form Loss Multiplier	5-3
6.	QUALIFICATION WITH ANALYTIC SOLUTIONS	6-1
7.	COMPARISONS WITH PLANT OPERATING DATA	7-1
8.	CONCLUSIONS	8-1
9.	REFERENCES	9-1
APPENDIX A	LIST OF SYMBOLS	A-1

ACKNOWLEDGEMENTS

This code was developed by J. Lindner of ASEA-ATOM, Västerås, Sweden and obtained by Westinghouse Electric Corporation under a licensing agreement with ASEA-ATOM.

The author wishes to acknowledge the work provided by Kuo-Fu Chen on inserting the code into the Westinghouse computer system and in evaluating the analytic solution discussed in Section 6. He also acknowledges the many valuable comments and suggestions by R. P. Knott on the use and understanding of the code and on the review of this manuscript.

ABSTRACT

CONDOR is a thermal hydraulics computer code that calculates at steady state conditions the three dimensional distribution of coolant flow, enthalpy, pressure, void fraction, heat flux, CPR (critical power ratio) and other associated parameters in a BWR core. The basic models, correlations and methodology used in the core flow and enthalpy calculations are described. Comparisons are given between CONDOR predictions and plant process computer output.

1.0 INTRODUCTION

CONDOR, a digital code developed by ASEA-ATOM, Sweden, has been used for many years and has found wide application in the thermal hydraulic steady state design and analysis of a Boiling Water Reactor (BWR) core. It has been modified and verified by Westinghouse as appropriate for use in evaluation of performance and licensing basis analysis for BWR's designed in the United States. The code can model an individual fuel assembly, a partial or complete reactor core or the entire internal recirculation loop. CONDOR calculates the three dimensional steady state distributions of coolant flow, enthalpy, pressure, void fraction, heat flux, CPR (critical power ratio) and other associated items in the core. This is done using the conservation equations, the associated constitutive relations, and the specific channel input. This report presents a description of the code methodology, the correlation bases, a qualification with an analytic solution and comparisons with plant process computer output.

2.0 GENERAL DESCRIPTION OF CONDOR CODE

2.1 Purpose

The CONDOR code was developed to determine the steady state distribution of coolant flow, enthalpy, pressure, void fraction, CPR (critical power ratio) and other associated items within a BWR core. The code has the capability to model a single fuel assembly or channel, a partial or total core or the entire primary coolant loop. The flows and heat transfer in the bypass regions can be explicitly modeled. The code description given in this report will only address the analysis of the core.

2.2 Brief Description of Core Analysis

The code has the capability of analyzing the entire primary loop of a BWR. Figure 2.1 gives a flow diagram for the entire loop. There are many options available to run the code through the proper choice of input data. The option described herein considers that the total coolant flow is given and the core flow distribution is calculated.

The core is divided into a group of parallel vertical flow channels. Each channel is axially subdivided into a number of nodes. The total power, total flow, inlet temperature or enthalpy, system pressure, axial and radial power distributions, geometries and component pressure loss coefficients are input. The code then iterates on the flow distribution among the channels until a converged solution is obtained. Single and two phase water properties are evaluated from incorporated standard international functions.[1] The converged solution consists of the three dimensional distribution of coolant flow, enthalpy, pressure, void fraction, CPR and other associated parameters within the core. Figure 2.2 gives a schematic of the CONDOR core flow distribution model.

CONDOR uses the conservation equations and required constitutive relations and correlations, e.g. void and pressure drop correlations and steam tables to obtain the solution. The local steam/water properties are evaluated using the local coolant pressure of the calculational node. The flow regimes represented are single phase water, subcooled boiling and bulk boiling.

The assumptions used to obtain the solution are

(i) Uniform static pressures at core inlet and outlet.

(ii) One dimensional vertical upward flow in each core channel.

(iii) No flow communication between heated flow channels in the core.

(iv) Uniform inlet enthalpy.

The flow in each channel is thus dependent on the power of the channel and the hydraulic characteristics of the channel.

The CONDOR code is used to obtain the steady state flow and enthalpy distribution within a core. Some of the applications of the solution are:

(i) The coupling of the CONDOR code with the neutronics code POLCA[2] through the power void iteration.

(ii) Determination of the thermal limits (MCPR) for safety evaluations.

(iii) Initial and final statepoints conditions for transients.

(iv) Pressure loadings on internal structures, e.g. channels, core plates, etc.

(v) Determination of design parameters such as bypass flow rates.

001354.13

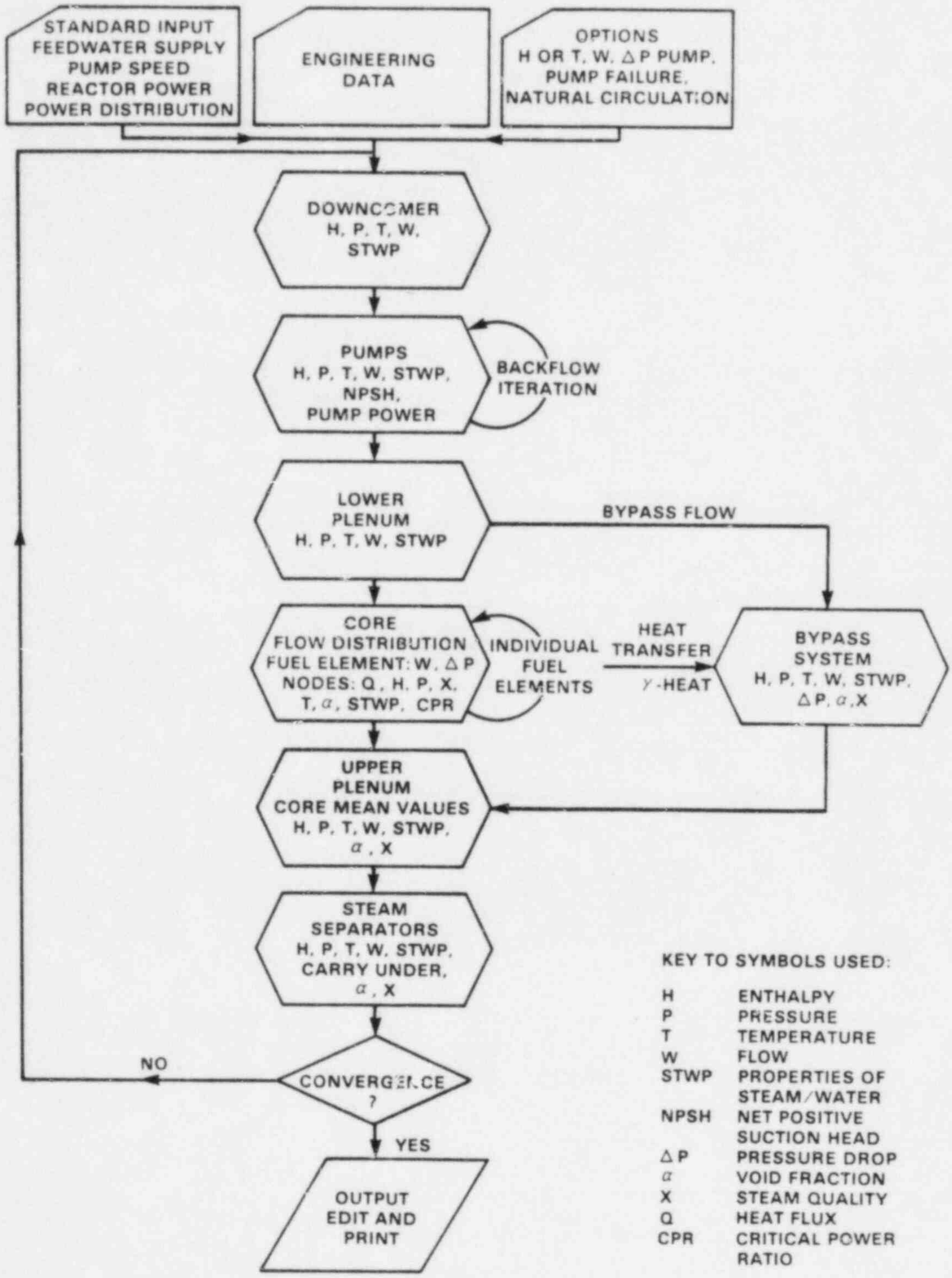

KEY TO SYMBOLS USED:

H	ENTHALPY
P	PRESSURE
T	TEMPERATURE
W	FLOW
STWP	PROPERTIES OF STEAM/WATER
NPSH	NET POSITIVE SUCTION HEAD
ΔP	PRESSURE DROP
α	VOID FRACTION
X	STEAM QUALITY
Q	HEAT FLUX
CPR	CRITICAL POWER RATIO

Figure 2.1 Condor Flow Chart

001517-2

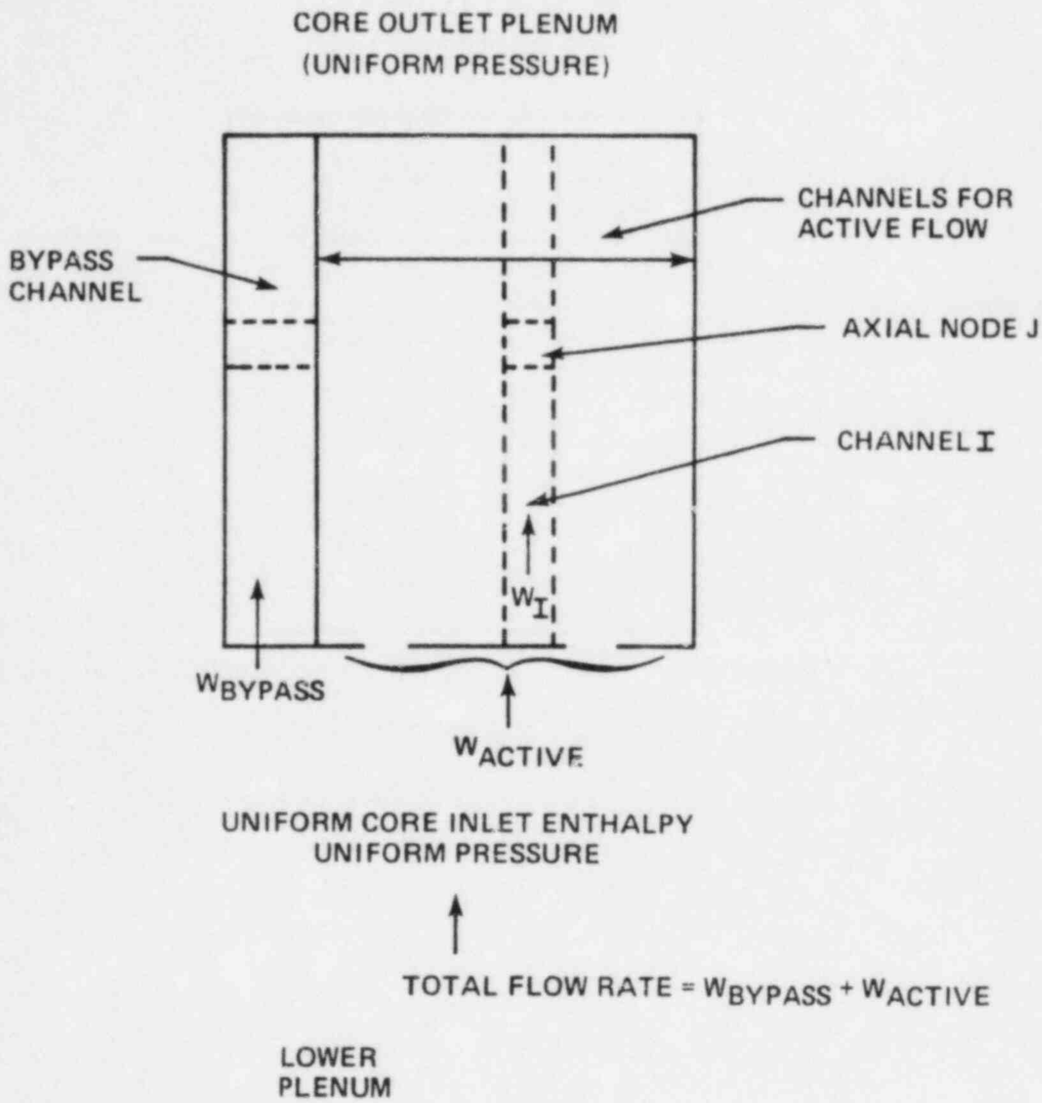

Figure 2.2 Schematic of CONDOR Core Flow Distribution Model

3.0 CONDOR METHODOLOGY

3.1 Introduction

This section describes the methodology used to solve for the flow, enthalpy, void distribution and other associated parameters in a BWR core. This includes the conservation equations and associated constitutive relations and correlations, the bypass flow models and the solution technique.

3.2. Conservation Equations

3.2.1 Continuity

CONDOR treats the core as a group of parallel channels connected to inlet and outlet plenums with no crossflow or mixing between the channels. Thus continuity is satisfied by having the sum of the flows from all core channels equal to the total flow to the core.

3.2.2 Energy

For the normal analysis of a core the heat input to a given channel axial node divided by the flow rate is equal to the enthalpy rise for that channel node.

CONDOR has the option to calculate the heat transfer across the fuel channel wall from the active flow to the bypass flow. If this is done, then the code accounts for this heat transfer in the energy balance for each axial node of each flow channel.

3.2.3 Momentum

The momentum equation for a given channel can be written as

$$\Delta P_{total} = \Delta P_{el} + \Delta P_{acc} + \Delta P_{fric} + \Delta P_{local} \qquad (3.1)$$

where

ΔP_{total} = total pressure drop over the axial node ΔZ,

ΔP_{el} = elevation pressure drop

ΔP_{acc} = acceleration pressure drop

ΔP_{fric} = friction pressure drop

ΔP_{local} = local pressure drop (e.g. orifice, spacer)

The individual expressions for each of these are given in the remainder of this section.

(i) Elevation

$$\Delta P_{el} = g \cdot \Delta Z \cdot (\rho_f - \alpha_m(Z) \cdot \Delta\rho) \quad (3.2)$$

where

g = gravitational constant

$Z, \Delta Z$ = axial distance or node length

ρ_f = density of saturated liquid. (At subcooled conditions ρ_f = density of subcooled liquid.)

α_m = mean void fraction in the node

$\Delta\rho$ = density difference between saturated phases

(ii) Acceleration

$$\Delta P_{acc} = \left[\frac{G^2}{\rho_f} \cdot \phi_A^2\right]_Z - \left[\frac{G^2}{\rho_f} \cdot \phi_A^2\right]_{Z-1} \quad (3.3)$$

where

G = mass flux

ϕ_A^2 = acceleration multiplier.

$$= \frac{[1 - X_a(Z)]^2}{1 - \alpha(Z)} + \frac{[X_a(Z)]^2 \cdot \rho_f}{\alpha(Z) \cdot \rho_g} \quad (3.4)$$

X_a = actual steam quality

ρ_g = density of saturated vapor.

For single phase flow $\phi_A^2 = 1$.

(iii) Friction

$$\Delta P_f = \frac{G^2}{2\rho_f} f \frac{\Delta Z}{D_e} \phi^2 \quad (3.5)$$

where

f = single phase friction factor

D_e = hydraulic diameter

ϕ^2 = two phase friction multiplier

The single phase friction multiplier is given by

$$f = \max\left[C/Re,\ A\ Re^{-B}\right] \qquad (3.5)$$

where

A, B, C = empirically determined constants

Re = Reynolds number

The equations and bases for the single phase friction factor and the two phase friction multiplier are given in Section 5.

(iv) Local

$$\Delta P_{local} = \frac{G^2}{2\rho_f} K \cdot \phi^2_{loc} \qquad (3.7)$$

where

K = single phase local (form) loss coefficient

ϕ^2_{loc} = two phase form loss multiplier

The equations and bases for K and ϕ^2_{loc} are given in Sections 5 and 7

3.3 Void Models

The void fractions calculated in CONDOR are directly used in the pressure drop evaluations. These void fractions are also used in the neutronics code POLCA when coupled with CONDOR. The CONDOR void fraction models consider both detached subcooled boiling and bulk boiling. The equations and bases for these models are given in Section 4.

3.4 Bypass Flow Models

The bypass flow paths consist of various leakage paths from the lower plenum and fuel assembly inlet plenum to the vertical heated flow channels formed by the fuel channel walls, as illustrated in Figure 3.1. Normally the leakage flows will be specified as a function of total flow rate. However, CONDOR has the option to explicitly calculate the bypass flow rates. The equations in CONDOR to do this can be expressed as

$$W = C_1 + C_2 \Delta P^{1/2} + C_3 \Delta P^{C4} \tag{3.8}$$

where

W = flow through the leakage flow paths.

ΔP = pressure drop across the leakage flow path from the lower plenum or fuel assembly inlet plenum to the core outlet

C_1, C_2, C_3, C_4 = constants

The leakage flow enters the bottom of the vertical heated bypass flow channels and exits at the core outlet. The description of the thermal hydraulics of these channels follows that described in the earlier sections. The CONDOR code can consider both heat generation in the bypass channel (gamma heating) and heat transfer across the channel walls from the active flow. The heat transfer coefficient for this can be written as.

$$K_{BP} = \frac{1}{\frac{1}{h_{BOX}} + \frac{S_{BOX}}{K_{BOX}} + \frac{1}{h_{BP}}} \tag{3.9}$$

where

K_{BP} = heat transfer coefficient between active and bypass flows

h_{BOX} = the heat transfer coefficient between active coolant and channel wall

K_{BOX}/S_{BOX} = the heat conductance through the channel wall

h_{BP} = the heat transfer coefficient from channel wall to bypass coolant.

The heat transfer coefficient h_{BOX} between active coolant and channel wall is based upon the Dittus-Boelter correlation[3] when the active coolant flow is single phase or subcooled boiling:

$$K_{BOX} = \frac{K_f}{D_e}\ 0.023\ Re^{.8} Pr^{.4} \qquad (3.10)$$

+

(a,c)

3.5 Solution Technique

The solution technique used by CONDOR to solve the core flow distribution from a given total flow, power distribution and inlet enthalpy is summarized below.

(1) The core and bypass region are divided into a given number of coolant channels with given inlet conditions. The power to each channel is given. Each channel is axially subdivided into a number of nodes.

(2) An initial guess is made by the code for the flow to each individual coolant channel.

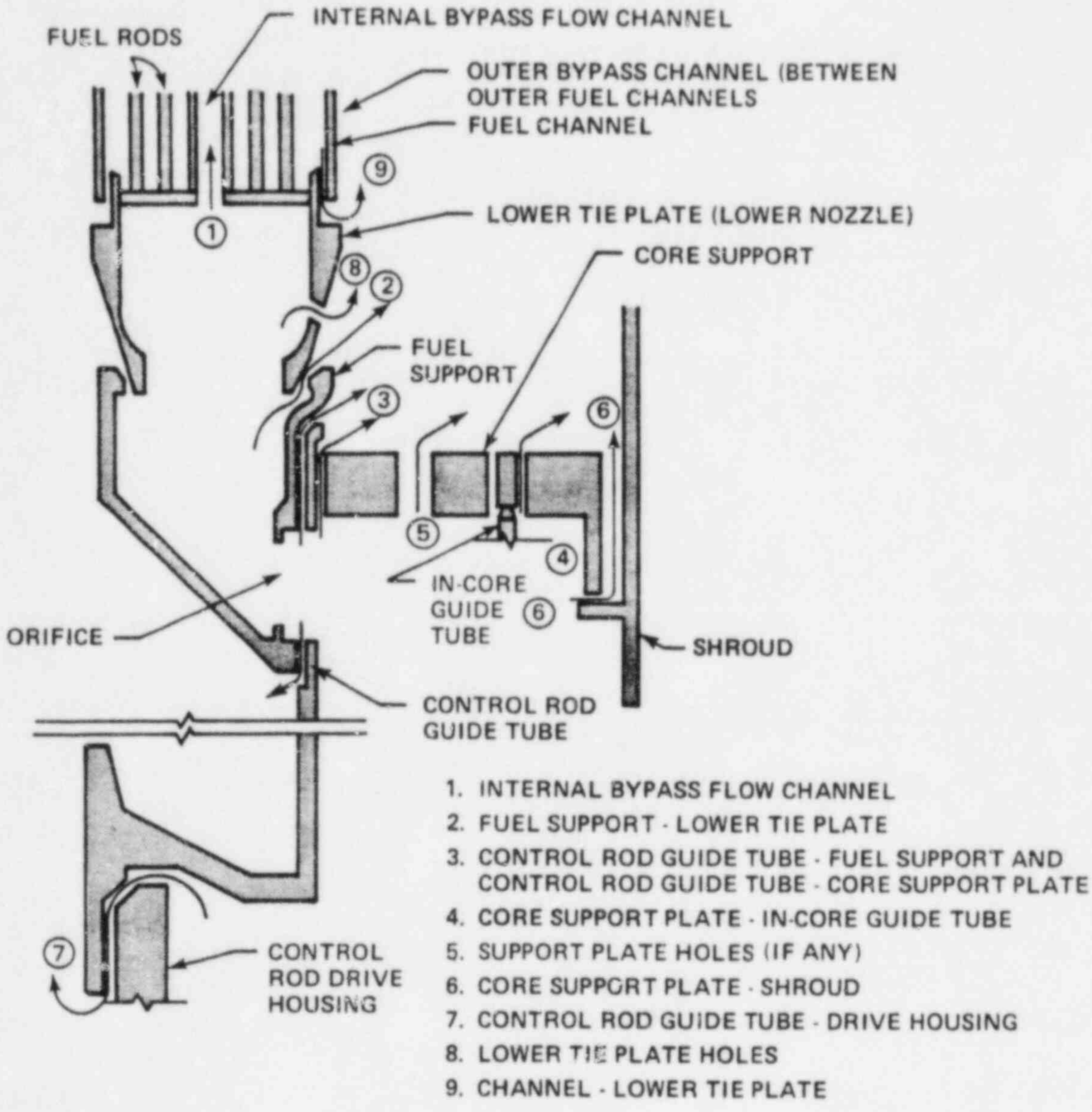

Figure 3.1. Schematic of Bypass Flow Paths

(3) An approximate pressure drop - flow relationship is set up for every channel modeled in the core.

(4) The flows for every channel are calculated from the approximate pressure drop-flow relationship.

(5) Using the flows from (4) the pressure drop, qualities, voids, etc. are now calculated from the conservation and associated equations described in the previous sections. These calculations proceed stepwise along each axial node from inlet to outlet for each channel. When the calculations in a node are completed the results are used as input data to the next node.

(6) Using the pressure drops from (5), steps (3), (4) and (5) are repeated until a converged solution using a criteria on the pressure drops, is obtained. The scheme converges rapidly (usually 2 to 4 iterations). Thermal margins are calculated during the final iteration.

4.0 VOID MODELS

The void fraction in forced convection two phase boiling can be divided into three regions as illustrated in Figure 4.1. Region I consists of voids traveling in a narrow bubble layer close to the wall. Region II starts at the point Z_0 where the bubbles are detached into the subcooled core and Region III starts at the point Z_1 where the bulk temperature reaches the saturation temperature and thermodynamic equilibrium is attained. The void fraction model in CONDOR (i) neglects the void fraction in Region I, (ii) uses the Levy model [6] to predict the void departure point in Region II and, (iii) in Region III uses a model based on the formulation of Zuber [7] with coefficients adjusted to give agreement with test data.

4.1 Levy's Model (Detached Voidage)

Levy's model [6] is used to predict the local subcooling at the bubble departure point. The expression for ΔT, the local subcooling at the bubble departure point, is given by

[ ]+

(a,c,g)

+

(a,c,g)

4.2 Bulk Boiling

The void model used to predict the void fraction in the bulk boiling region is based on that developed by Zuber et. al.[7]. The void-quality expression in this region can be written as

$$\alpha = \frac{X_a}{Co \frac{\Delta\rho}{\rho_f} X_a + [Co + \frac{V_{gi}}{W_f}] \frac{\rho_g}{\rho_f}} \tag{4.2.1}$$

where Co is the concentration parameter

V_{gi} = drift velocity

W_f = inlet liquid velocity at saturation temperature.

The parameters Co and V_{gi} are determined from experimental data.

[ ]+ (a,c,g)

2120F:6/831209

+

(a,c,g)

The coefficients in the equations above were determined based on data from two sets of experiments on 36 rod bundles. The comparisons of the predictions to the data are shown in Figures 4.2, 4.3 and 4.4. The letters denote the various pressures at which the data was taken. The correlation above was compared to 3 other sets of data taken from both a 36 rod bundle and 64 rod bundles. A summary of the comparison of all of the above data to predictions is given in Table 4.1. It is seen that there is excellent agreement between the measurements and the model predictions.

Measurement Series	Number of Measurements	Average Error %	Standard Deviation %
FT36B, 30 bar	51	5.5	6.2
50	93	3.2	3.4
70	51	1.3	3.6
87	13	4.2	5.2
OF 36, 30 bar	53	2.7	4.1
50	52	2.6	2.8
70	253	.4	3.4
90	48	-.5	3.4
FT36C, 30 bar	34	3.1	4.2
50	181	1.5	3.7
70	44	.5	3.4
OF 64A,48 bar	69	2.3	2.9
68	223	1.4	2.4
OF 64B,68 bar	182	-1.6	2.3
Total	1347	1.2	3.7

TABLE 4.1 COMPARISON OF DATA TO PREDICTIONS

001354.14

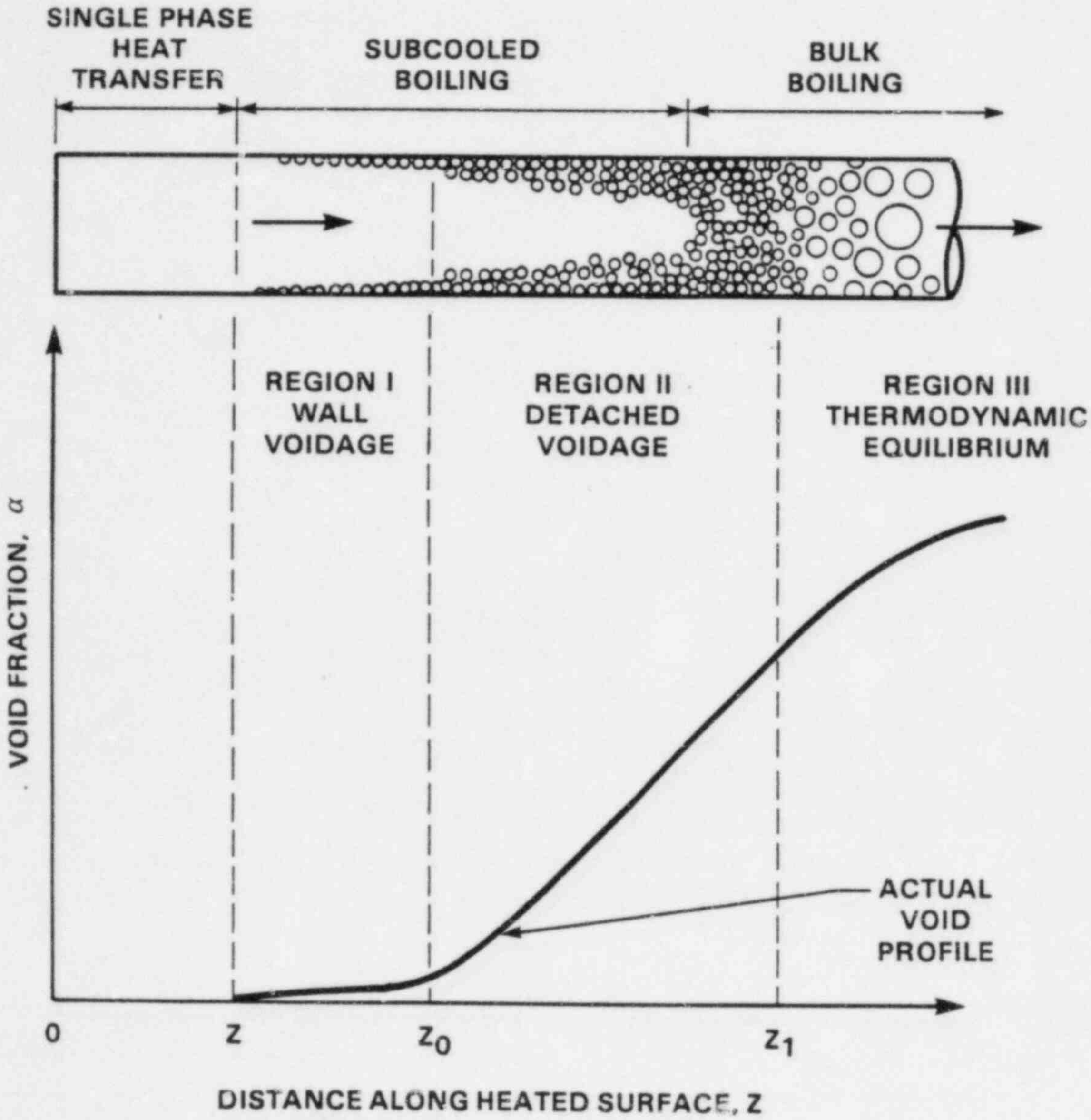

Figure 4.1 Two Phase Flow Boiling Regions

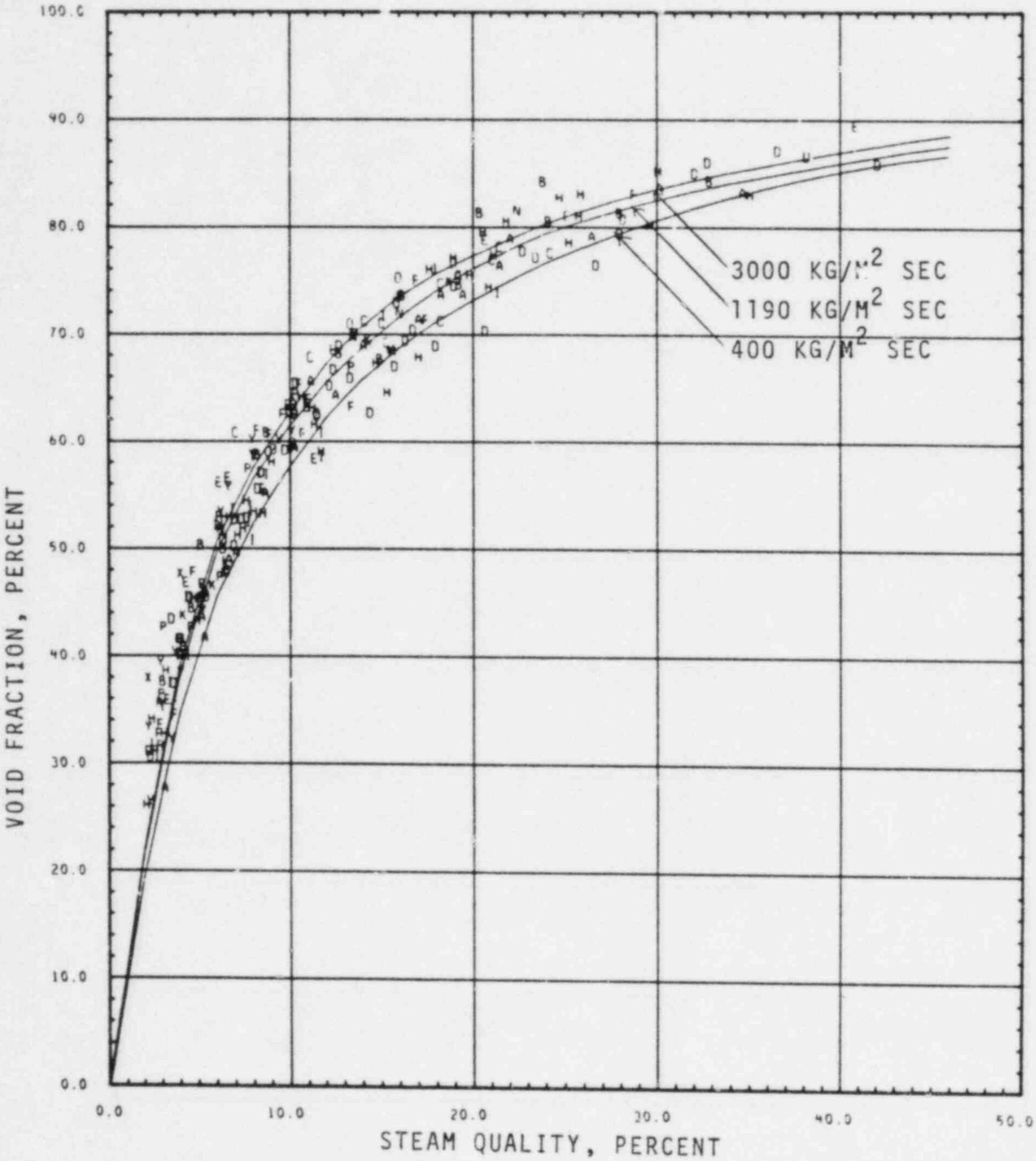

FIGURE 4.2 - COMPARISON OF VOID MODEL WITH DATA

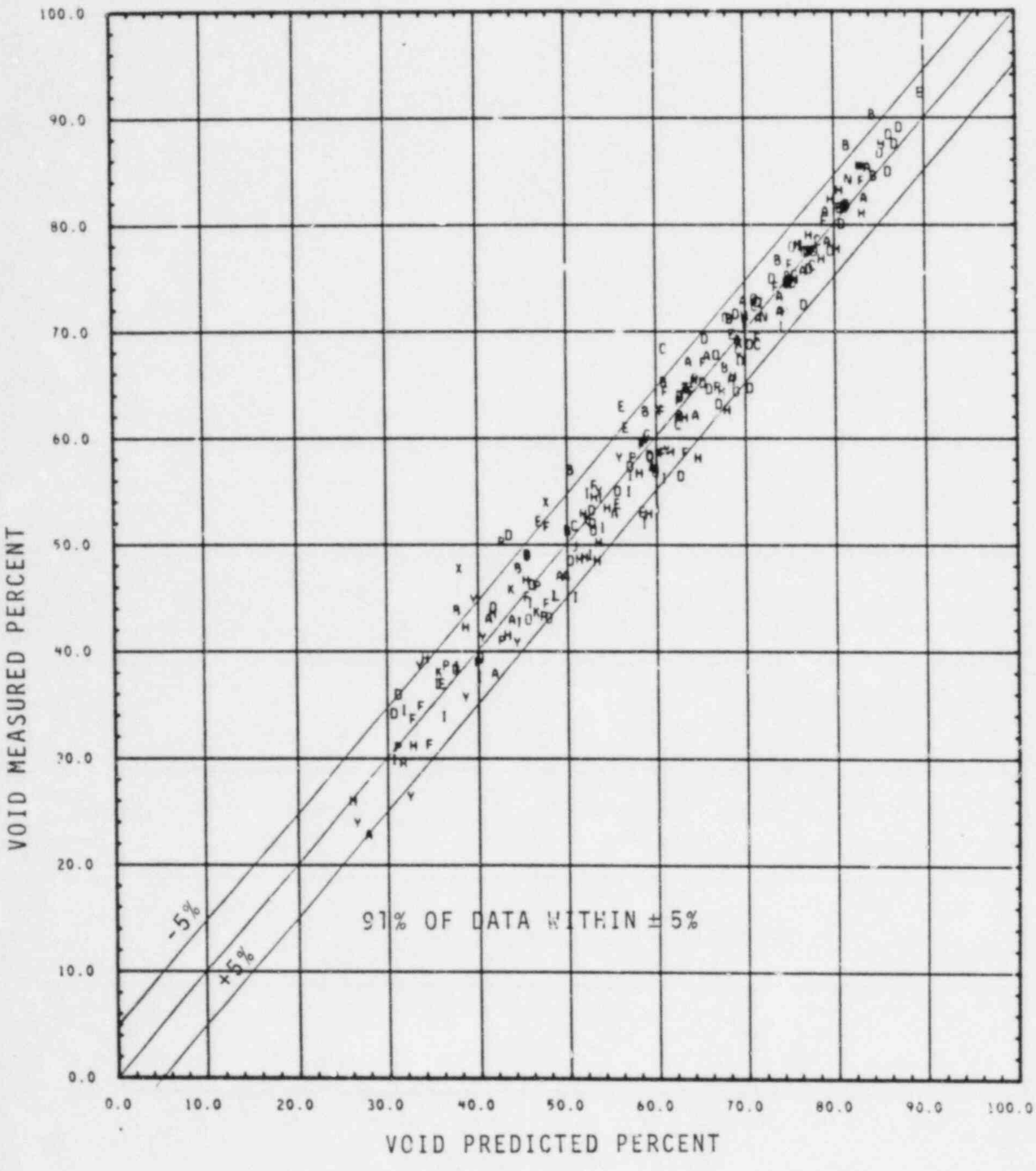

FIGURE 4.3 - COMPARISON OF VOID MODEL WITH DATA

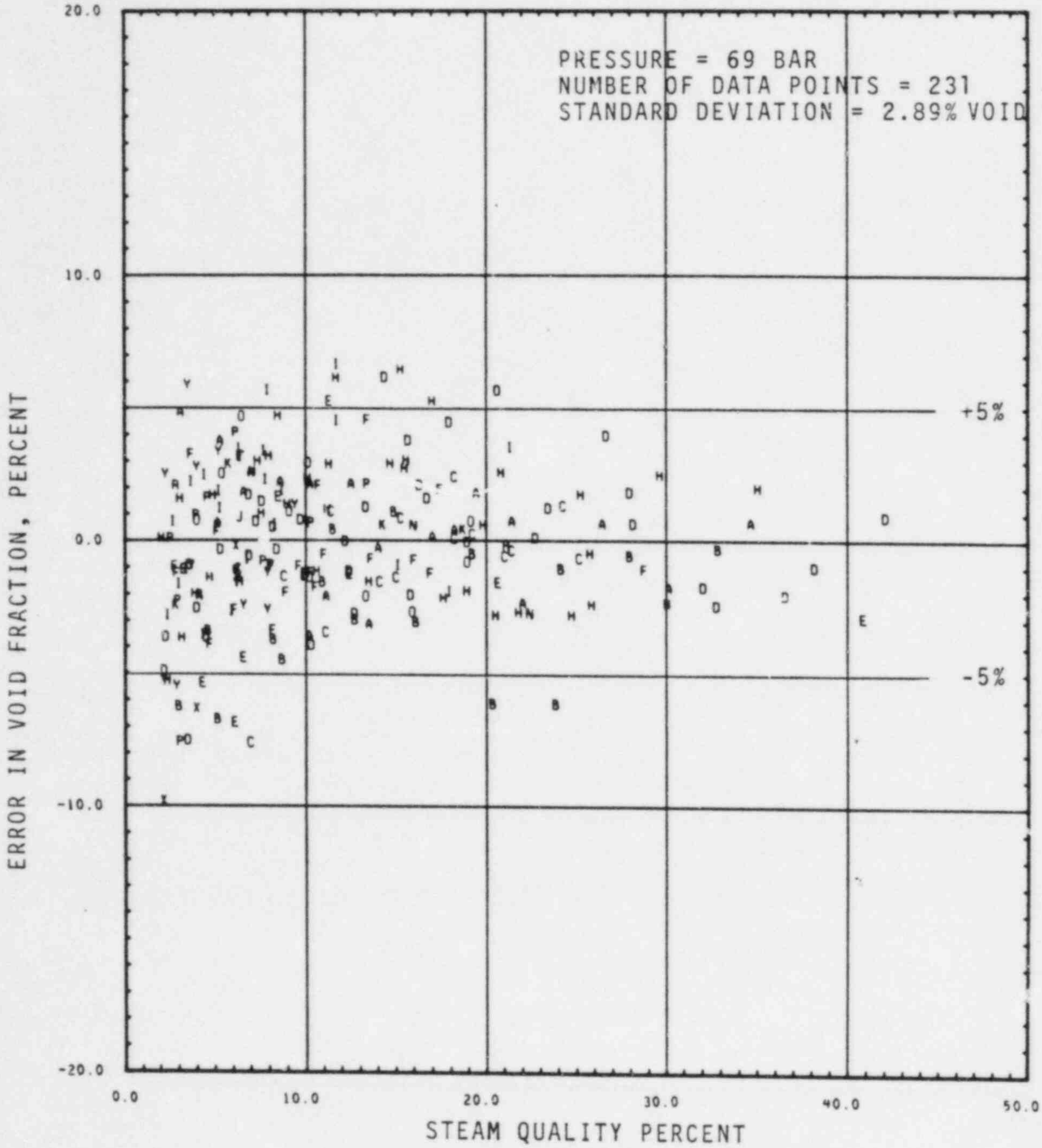

FIGURE 4.4 - COMPARISON OF VOID MODEL WITH DATA

5.0 PRESSURE DROP CORRELATIONS

5.1 Introduction

The basic equations for the various pressure drop components were given in Section 3.2.3. The equations and bases for the single and two phase friction and form (local) multipliers are given in the following Sections.

5.2 Single Phase Friction

The single phase friction factor f is predicted by the Blasius equation

$$f = A/Re^{B}$$

where Re = Reynolds number

A, B = input constants

Typically A and B are both taken to be 0.2. These values have been confirmed by measurements in single phase rod bundle tests.

5.3 Two Phase Friction

The two phase friction multiplier used in design is based on the Baroczy[9] and Chisholm[13] correlations modified using two phase 64 rod bundle pressure drop data. The form of this correlation is:

+

(a,c,g)

+

(a,c,g)

This correlation covers the following parameter ranges:

Pressure	1 to 100 bar
Mass velocity	1 to 3000 kg/m^2s
Quality	0 to 100 %W

A comparison of this correlation to its data base gives the following statistics.

Number of points	288
Mean deviation, %	0.3
Standard deviation,%	8.3

The detailed comparison of this correlation with its data base is given in Figure 5.1 and 5.2.

5.4 Single Phase Form

The single phase form loss coefficient K is used in the following equation to calculate the local pressure losses ΔP_{loc}:

$$\Delta P_{loc} = \frac{G^2}{2\rho_f} K$$

G = mass flux.

ρ_f = density of saturated liquid (At subcooled conditions, ρ_f = density of subcooled liquid)

5.5 Two Phase Form Loss Multiplier

†

(a,c,g)

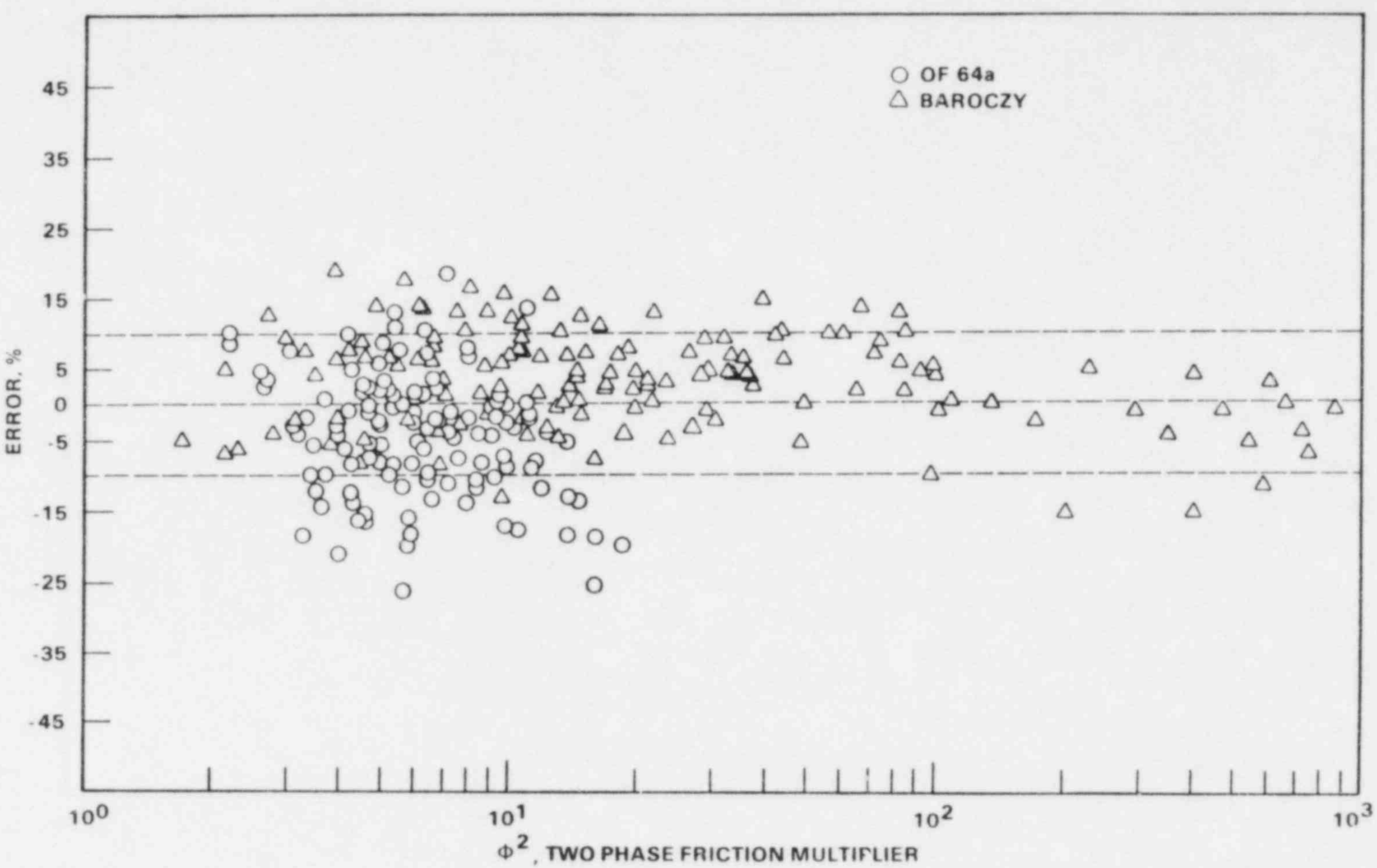

001354.16

Figure 5.1 Two Phase Friction Multiplier Compared to OF64a Data and BAROCZY

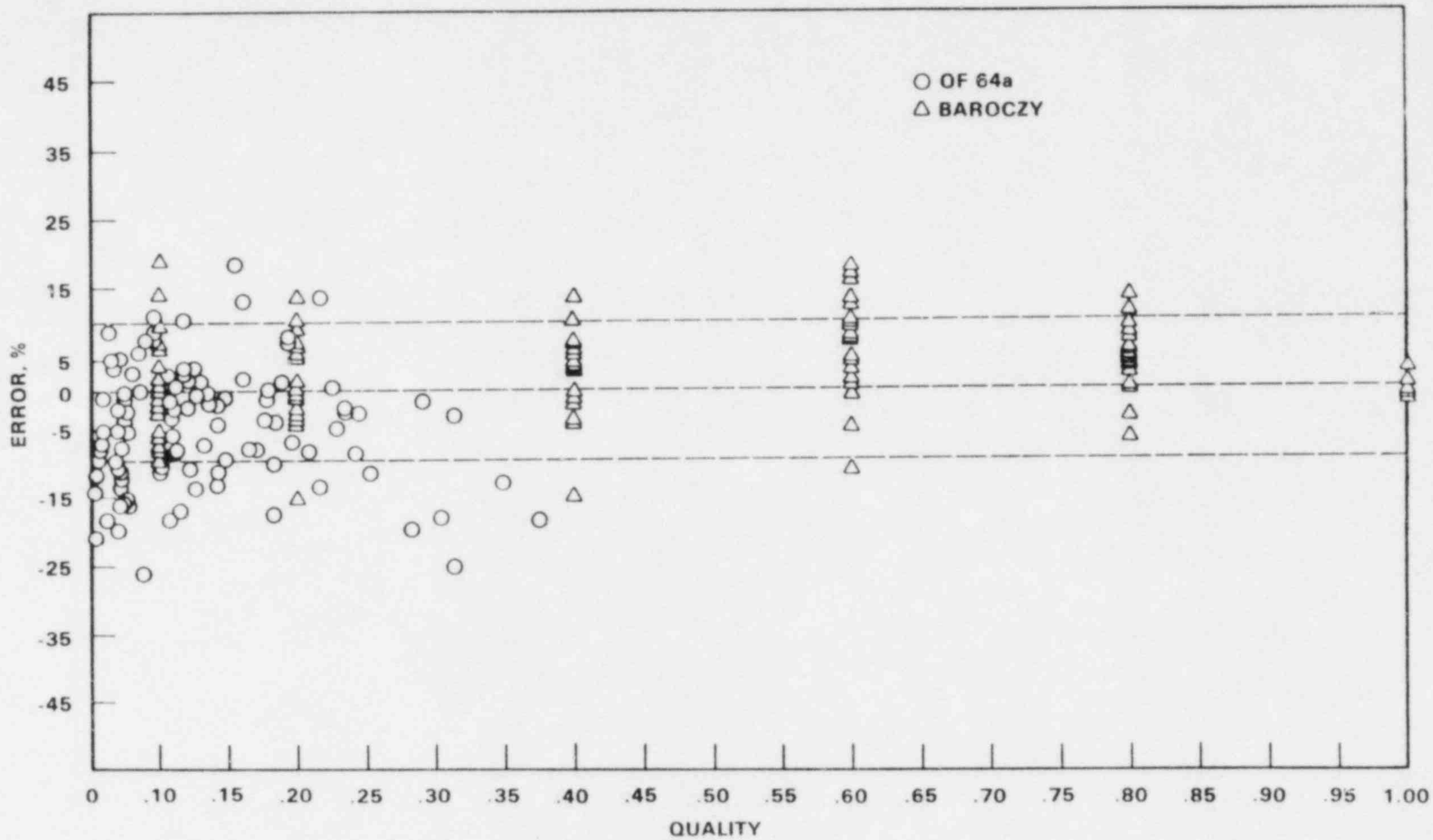

Figure 5.2 Two Phase Friction Multiplier Compared to OF64a Data and BAROCZY

001354.15

6.0 QUALIFICATION WITH ANALYTIC SOLUTIONS

A verification of the CONDOR code can be made by comparing CONDOR predictions to those of two analytic solutions. The first, which was for the case of homogeneous equilibrium two phase flow in a vertical heated tube with uniform heat flux, was derived in Reference 10. The second, an extension of the first to a cosine axial power shape, is derived further on in this Section. Starting with the first, the momentum equation (3.1) can be written as

$$\Delta P_{total} = \Delta P_{acc} + \Delta P_{fric} + \Delta P_{el} + \Delta P_{local}$$

where

$$\Delta P_{acc} = G^2 \int_0^{L_H} \frac{d}{dZ} \frac{1}{\rho_m} \, dZ \tag{6.1}$$

$$\Delta P_{fric} = \frac{G^2 f}{2\rho_f De} \int_0^{L_H} \phi^2 \, dZ \tag{6.2}$$

$$\Delta P_{el} = g \int_0^{L_H} \rho \, dZ \tag{6.3}$$

$$\Delta P_{local} = \sum \frac{G^2 K}{2\rho_f} \phi^2_{loc} \tag{6.4}$$

G = mass flux

Z = axial distance

L_H = heated length

K = single phase form loss coefficient

ϕ^2 = two phase friction multiplier

ρ = density

f = single phase friction factor

De = hydraulic diameter

$$\rho_m = \frac{1}{\dfrac{X_a^2}{\alpha \rho_g} + \dfrac{(1 - X_a)^2}{\rho_f (1 - \alpha)}}$$

X_a = flow quality

α = void fraction

g = acceleration due to gravity

Assuming thermal equilibrium and uniform heat flux, then $X_a = 0$ up to the bulk boiling initiation location λ, defined by

$$\lambda = \frac{GA_{X-S}\ \Delta H_{sub}}{P_H \cdot QA} \tag{6.5}$$

where

A_{X-S} = convectional flow area
ΔH_{sub} = inlet subcooling
P_H = heated perimeter
QA = heat flux

and X_a is a linear function of the elevation Z in the bulk boiling region

$$X_a = \frac{QA \cdot P_H \cdot Z}{G\ A_{X-S}\ H_{fg}} - \frac{\Delta H_{sub}}{H_{fg}} \tag{6.6}$$

The expression used to determine the void fraction α is given by the Zuber-Findlay relationship

$$\alpha(Z) = \frac{X_a}{Co\ (X_a + \frac{\rho_g}{\rho_f}(1 - X_a)) + \frac{\rho_g V_{gi}}{G}} \tag{6.7}$$

which we have simplified by setting Co = 1 and V_{gi} = o.

Equations (4.1 and (4.3) can be integrated to obtain

$$\Delta P_{acc} = G^2 \left[\frac{(1 - X(L_H))^2}{(1 - \alpha(L_H))\rho_f} + \frac{(X(L_H))^2}{\rho_g \alpha (L_H)} - \frac{1}{\rho_f}\right] \tag{6.8}$$

$$\Delta P_{el} = g \left\{ \rho_f L_H - (\rho_f - \rho_g) \left[(L_H - \lambda) \frac{F_1}{F_5} - \frac{F_3 F_1}{F_5^2} \ln\left[\frac{F_5 L_H + F_3}{F_5\lambda + F_3}\right] - \frac{F_2}{F_5} \ln \left[\frac{F_5 L_H + F_3}{F_5\lambda + F_3}\right]\right]\right\} \tag{6.9}$$

where

$$F_1 = \frac{QA \cdot P_H}{GA_{X-S}\ H_{fg}}$$

$$F_2 = \frac{\Delta H_{sub}}{H_{fg}}$$

$$F_3 = (1 + F_2) \frac{\rho_g}{\rho_f} - F_2$$

$$F_5 = F_1 \left(1 - \frac{\rho_g}{\rho_f}\right)$$

In order to integrate the frictional pressure drop term (4.2), the following approximation to the Martinelli-Nelson model for ϕ^2 is used

$$\phi^2 = C \left[1.2 \left(\frac{\rho_f}{\rho_g} - 1\right) X_a^{.824} \right] + 1 \qquad (6.10)$$

where

$$C = 1.36 + .0005\,p + .1\,G/10^6 - .000714\,p\,G/10^6$$

for $G < .7 \times 10^6$ lb/hr $\cdot$ ft^2

$$C = 1.26 - .0004\,p + .119\,10^6/G + .00028p\,10^6/G$$

for $G > .7 \times 10^6$ lb/hr $\cdot$ ft^2

p is in psia and G is in lb/hr $\cdot$ ft^2

Using this expression for ϕ^2, we obtain

$$\Delta P_{fric} = \frac{G^2 f}{2\rho_f D_e} \left[L_H + 1.2\,C\left(\frac{\rho_f}{\rho_g} - 1\right) \frac{(X_a\,(L_H))^{1.824}}{1.824 F_1} \right] \qquad (6.11)$$

The expression for the local losses can be evaluated using the homogeneous two phase multiplier.

$$\phi^2_{loc} = 1 + X_a \left(\frac{\rho_f}{\rho_g} - 1\right)$$

to obtain

$$\Delta P_{loc} = \sum \frac{G^2 K}{2\rho_f} \left[1 + (F_1 Z - F_2) \left(\frac{\rho_f}{\rho_g} - 1\right)\right] \qquad (6.12)$$

2120F:6/831209

Equations (6.8), (6.9), (6.11) and (6.12) can now be used to evaluate the pressure drop in a heated tube with a uniform axial power shape with the assumptions explicitly listed above and the further assumptions of no property changes (density, enthalpy) with axial location.

We now extend the above analytic solution to the case of a cosine axial power shape. Defining this shape as

$$QA = q_{max} \quad \mathrm{Cos} \frac{\pi}{L_H} (Z - L_H/2) \tag{6.13}$$

then the flow quality as a function of axial location Z is

$$X_a(Z) = \frac{L_H \; P_H \; q_{max}}{\pi \; GA_{X-S} \; H_{fg}} \quad \mathrm{Sin} \frac{\pi}{L_H} (Z - L_H/2)$$

$$+ \frac{L_H \; P_H \; q_{max}}{\pi \; GA_{X-S} \; H_{fg}} - \frac{\Delta H_{sub}}{H_{fg}}$$

This can be written as

$$X_a \; (Z) = F_6 \; \mathrm{Sin} \; \frac{\pi}{L_H} \; (Z - L_H/2) + F_7 \tag{6.14}$$

where

$$F_6 = \frac{L_H \; P_H \; q_{max}}{\pi \; GA_{X-S} \; H_{fg}}$$

$$F_7 = F_6 - \Delta H_{sub}/H_{fg}$$

After substituting (6.14) into (6.7) with $C_o = 1$ and $V_{gi} = 0$, the void fraction as a function of axial location is

$$\alpha = \frac{F_6 \; \mathrm{Sin} \; \frac{\pi}{L_H} (Z - L_H/2) + F_7}{F_8 \; \mathrm{Sin} \; \frac{\pi}{L_H} (Z - L_H/2) + F_9} \tag{6.15}$$

where

$$F_8 = (1 - \rho_g/\rho_f)\,F_6$$

$$F_9 = F_7 + (\rho_g/\rho_f)\,(1 - F_7)$$

The pressure drop due to acceleration was obtained by substituting equations (6.14) and (6.15) into equation (6.8). Equation (6.3) the elevation pressure drop can be integrated with $\rho = \rho_f - \alpha\,(\rho_f - \rho_g)$ to obtain

$$\Delta P_{el}\,(Z) = g\,\rho_f\,Z - g\,(\rho_f - \rho_g)\Bigg[\frac{F_6}{F_8}\,(Z - \lambda) + (F_7 - \frac{F_6\,F_9}{F_8})\,\frac{L_H}{\pi}\,\frac{1}{(F_8^2 - F_9^2)^{1/2}}\,x$$

$$\Bigg\{\log \frac{F_9 \tan((\pi/2L_H)(Z - L_H/2)) + F_8 - (F_8^2 - F_9^2)^{1/2}}{F_9 \tan((\pi/2L_H)(Z - L_H/2)) + F_8 + (F_8^2 - F_9^2)^{1/2}} -$$

$$\log \frac{F_9 \tan((\pi/2L_H)(\lambda - L_H/2)) + F_8 - (F_8^2 - F_9^2)^{1/2}}{F_9 \tan((\pi/2L_H)(\lambda - L_H/2)) + F_8 + (F_8^2 - F_9^2)^{1/2}}\Bigg\}\Bigg]$$

$$\text{for } |F_8| > |F_9| \qquad (6.16)$$

$$= g\,\rho_f Z - g\,(\rho_f - \rho_g)\Bigg[\frac{F_6}{F_8}\,(Z - \lambda) + (F_7 - \frac{F_6\,F_9}{F_8})\,\frac{L_H}{\pi}\,\frac{2}{(F_9^2 - F_8^2)^{1/2}}\,x$$

$$\Bigg\{\tan^{-1}\frac{F_9 \tan((\pi/2L_H)(Z - L_H/2)) + F_8}{(F_9^2 - F_8^2)^{1/2}}$$

2120F:6/831209

$$-\tan^{-1} \frac{F_9 \tan ((\pi/2L_H)(\lambda - L_H/2)) + F_8}{(F_9^2 - F_8^2)^{1/2}} \Bigg\} \Bigg]$$

$$\text{for} \left|F_8\right| < \left|F_9\right|$$

where

$$\lambda = \frac{L_H}{\pi} \, \text{Sin}^{-1} \left(\frac{GA_{X-S} \, \pi \, \Delta H_{sub}}{L_H \, P_H \, q_{max}} - 1 \right) + \frac{L_H}{2}$$

In order to integrate equation (6.2) the power of the quality in equation (6.10) was replaced by 1. The pressure drop due to friction as a function of Z then becomes

$$\Delta p_{fric} \, (Z) = \frac{f \, G^2}{2 \, \rho_f \, D_e} \Bigg\{ Z + 1.2 \, C \left(\frac{\rho_f}{\rho_g} - 1\right) x$$

$$\Bigg[F_7 \, (Z - \lambda) + \frac{F_6 \, L_H}{\pi} \Big\{ \cos \frac{\pi}{L_H} \left(\lambda - \frac{L_H}{2}\right)$$

$$- \cos \frac{\pi}{L_H} \left(Z - \frac{L_H}{2}\right) \Big\} \Bigg] \Bigg\} \qquad (6.17)$$

The pressure drop due to the spacer grid was obtained by substituting equation (6.14) into ϕ^2_{loc}.

The two analytic solutions given above for uniform and cosine axial power shapes were used to evaluate the pressure drop in a tube at inlet and system pressure of 1000 psia over a large range of exit flow qualities.

The CONDOR code was set up to evaluate the above problems. To do this the void fraction expression in the above analytic solution and two phase friction multipliers equal to the above expressions were inserted into the code. There is a small difference between the analytic solution and the CONDOR evaluations since CONDOR evaluates the local steam/water properties using the local coolant pressure of the calculational node whereas the analytic solutions is based on evaluation of these properties based on a given constant system pressure. The effect of this is insignificant for small variations in pressure.

The comparison between the analytic solutions and the CONDOR predictions are shown in Figure 6.1 for the uniform power shape and Figure 6.2 for the cosine axial power shape. It is seen that there is excellent agreement over the entire parameter range for both the total pressure drop and the individual components of the pressure drop.

1517

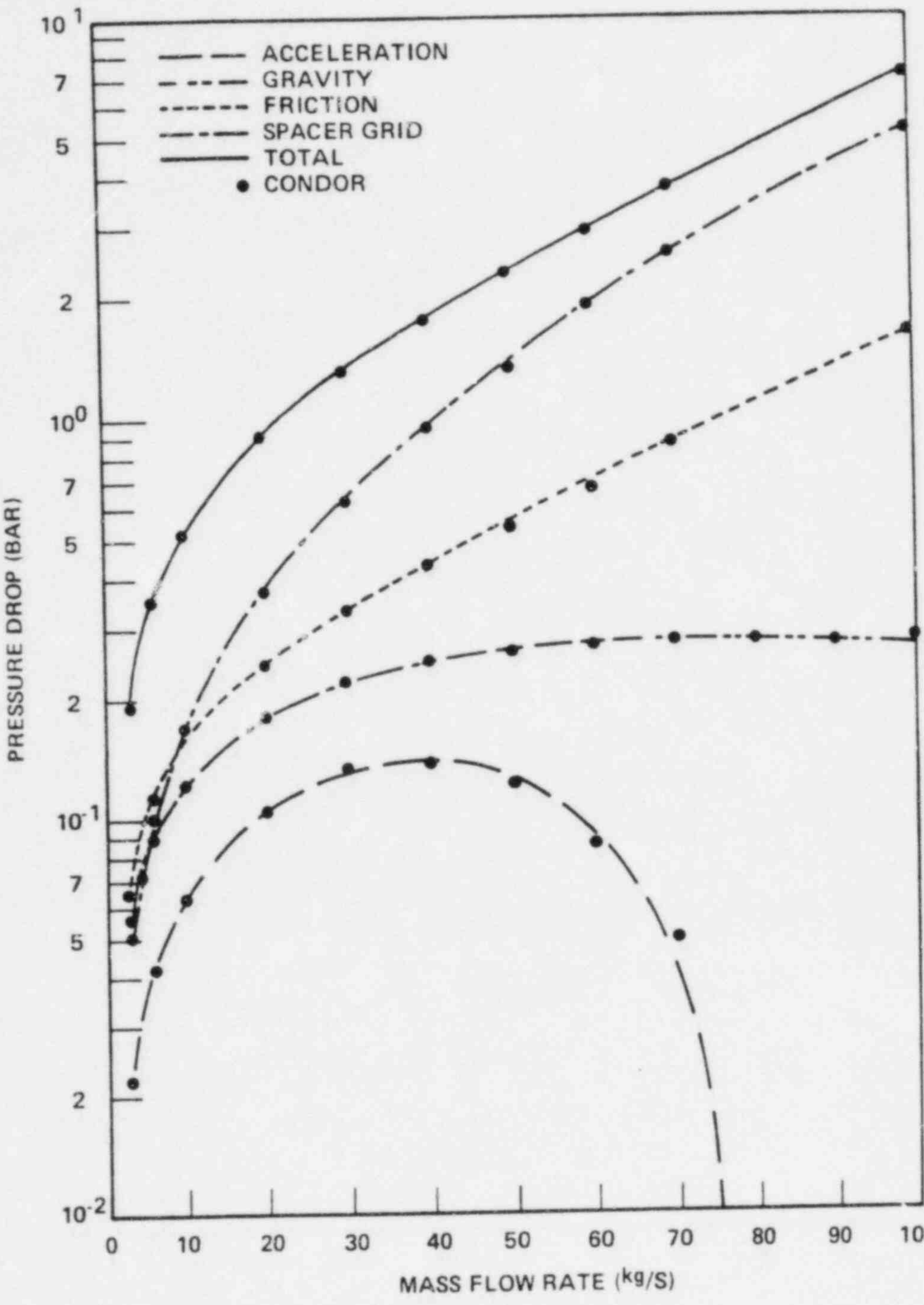

Figure 6.1. CONDOR Pressure Drop Predictions Compared to Analytic Solution

1517-4

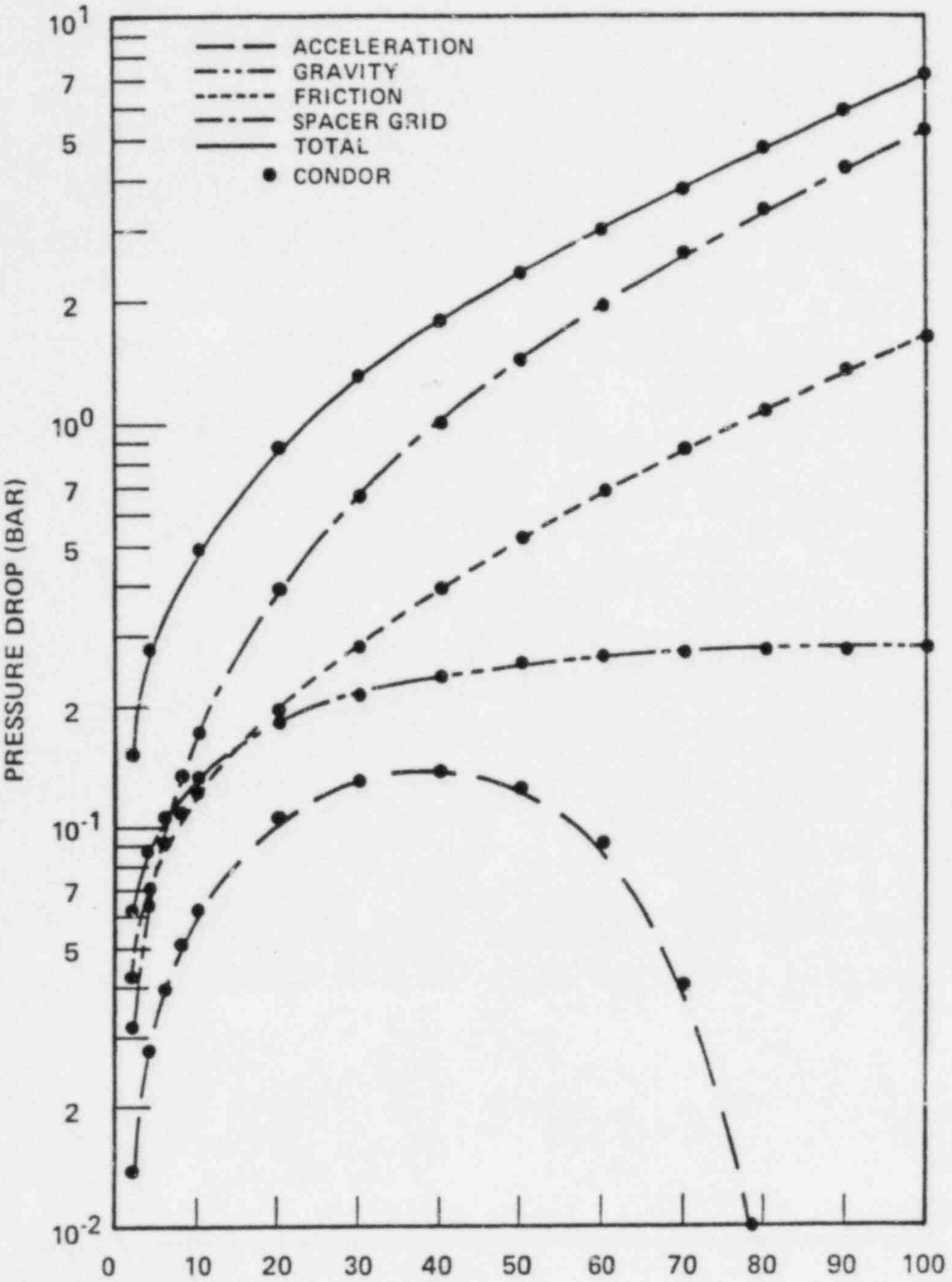

Figure 6.2. CONDOR Pressure Drop Predictions Compared to Analytic Solution - Cosine Axial Power Shape

7.0 COMPARISONS WITH PLANT OPERATING DATA

CONDOR models were developed to analyze the [ ]+ core. Predictions from these models were compared to the P1 process computer output. CONDOR calculates the flow and enthalpy distribution in the core. An accurate calculation of the flow and enthalpy in the hot assembly helps to ensure that the MCPR of the core is accurately calculated. Quarter core symmetry was assumed. Two CONDOR models were used. The first was a detailed model with every fuel assembly modeled by a separate channel. The second CONDOR model lumped together all channels having the same geometry characteristics, i.e. 8X8R central orificed, 8X8 peripheral orificed and 8X8 central orificed and an additional channel representing the hot fuel assembly. (a,c)

Table 7.1 identifies the fuel assembly types and gives the rated conditions for the cycle 3 core. The radial and axial power distributions, total flow, bypass flow fractions, dome pressure and inlet subcooling were obtained from the process computer output for each case run. Two percent of the heat generation was assumed to go to the bypass with no heat transfer across the fuel channel walls.

Table 7.2 gives the single phase form loss coefficients used in the analysis. The values in Table 7.2 (I) for the 8X8R fuel assembly were obtained from measurements taken from an unirradiated 8X8RP fuel assembly at the [ ]+ site. The measurements were taken using the W portable test loop FACTS (Fuel Assembly Compatiblity Test System). (a,c)

It is not possible to separate the orifice and lower tie plate losses in the test loop because they are interdependent. For the purposes of this calculations an approximate value of the the ratio of the lower tie plate to orifice loss coefficient for the central orifice was used in order to obtain the separate values. The values of the orifice and lower tie plate loss coefficients in the peripheral assemblies were

[ ]+ (a,c)

peripheral orifice. The orifice and lower tie plate loss coefficients given in Table 7.2 have been adjusted to account for the fraction of bypass flow that goes through the orifice.

The spacer and upper tie plate loss coefficients given in Table 7.2 (I) were obtained by using the [ ]+ (a,c)

Table 7.3 shows the results of the CONDOR evaluations of the core pressure drops and hot (highest powered central orificed) fuel assembly flow and outlet quality using the detailed 140 channel CONDOR model. The P1 cases were randomly selected from the cycle 3 output. It is seen that although the [ ]+ (a,c) Table 7.4 shows the results of a larger number of P1 values using the less detailed 4 channel CONDOR model. [ ]+ (a,c)

The cases given in Tables 7.3 and 7.4 were rerun using the spacer and upper tie plate loss coefficients given in Table 7.2 (II). The results of these evaluations are given in Tables 7.5 and 7.6. [ ]+ (a,c) Accurate prediction of the hot channel flow and qualities helps to ensure accurate prediction of the MCPR (minimum critical power ratios) used in safety evaluations.

It is seen from the above that the CONDOR code using values of the loss coefficients based on [ ]+ (a,c)

[ ]+ This could be due to (a,c)
effects that occur during reactor operation, e.g. crud buildup, or could be due to a bias in measurements such as coolant flow rate.

CONDOR predictions using the values of loss coefficients obtained from [ ]+ gave core pressure drops [ ]+ (a,c)

Accurate prediction of these latter two quantities for the hot assembly ensures accurate prediction of the MCPR.

Table 7.1 [ ]+ Core (a,c)

Rated power, Mwt.	[ ]+
Rated flow, lb/hr.	(a,c)

	8X8	8X8R
Number of 8X8R central orificed		
Number of 8X8 central orificed		
Number of 8X8 peripheral orificed		
Active fuel length, inch		

[ ]+ (a,c)

Table 7.2

Form Loss Coefficients Used in the CONDOR Analysis of [ ]+ (a,c)

(I) Loss Coefficients Based on FACTS Test Analysis of Clean Unirradiated 8X8RP Fuel Assembly

	8X8R	8X8	
Central orifice			
Peripheral orifice			(a,b,c)
Lower tie plate			
Spacer			(a,b,c)
Upper tie plate			

(II) Spacer and Upper Tie Plate Loss Coefficients based on [ ]+ (a,c)

	8X8R	8X8	
Spacer			(a,c)
Upper tie plate			

Loss coefficients based on bare rod bundle flow area.

Table 7.3 CONDOR Predictions for [ ]+ (a,c)

140 channel model of core (quarter core symmetry).
Loss coefficients from Table 7.2 (1)

	CONDOR	P1	P1 - CONDOR	
CORE PRESSURE DROP ,PSI				
(97.1% POWER/90.7%FLOW)	[		]+	
(88.0% POWER/72.2% FLOW)				(a,c)
(99.7% POWER/99.7% FLOW)				
HOT CHANNEL FLOW, LB/HR				
(97.1% POWER/90.7%FLOW)	[		]+	
(88.0% POWER/72.2% FLOW)				(a,c)
(99.7% POWER/99.7% FLOW)				
HOT CHANNEL OUTLET QUALITY, FRACTION				
(97.1% POWER/90.7%FLOW)	[	]+		
(88% POWER/72.2% FLOW)				(a,c)
(99.7% POWER/99.7% FLOW)				

Table 7.4 CONDOR Predictions for [ ] (a,c)

4 Channel model of core (quarter core symmetry).
Loss coefficients from Table 7.2 (I)

POWER/FLOW (%/%)	ΔP CORE CONDOR	ΔP CORE P1	ΔP CORE P1 - ΔP CORE CONDOR	HOT ASSEMBLY CHARACTERISTICS W P1	W CONDOR	X P1	X CONDOR
88.0/72.2							
75.1/86.7							
95.8/95.2							
97.2/93.7							
99.6/90.8							
99.5/83.6							
94.5/88.6							
76.3/67.4							
24.8/27.4							
99.7/99.7							
97.1/90.7							
50.4/44.7							

[ ]+ (a,c)

ΔP = Pressure drop, PSI

W = Assembly flow rate, 10^5 Lb/Hr

X = Assembly outlet quality, fraction

2120F:6

Table 7.5 CONDOR Predictions for [ ]+ (a,c)

140 Channel model of core (quarter core symmetry).
Loss coefficients from Table 7.2 (II)

	CONDOR	P1	P1 - CONDOR	
CORE PRESSURE DROP, PSI				
(97.1%/POWER/90.7% FLOW)	[		]+	
(88.0% POWER/72.2% FLOW)				(a,c)
(99.7% POWER/99.7% FLOW)				
HOT CHANNEL FLOW, LB/HR				
(97.1%/POWER/90.7% FLOW)	[		]+	
(88.0% POWER/72.2% FLOW)				(a,c)
(99.7% POWER/99.7% FLOW)				
HOT CHANNEL OUTLET QUALITY, FRACTION				
(97.1%'POWER/90.7% FLOW)	[		]+	
(88.0% POWER/72.2% FLOW)				(a,c)
(99.7% POWER/99.7% FLOW)				

Table 7.6 CONDOR Predictions for [ ]+ (a,c

4 Channel model of core (quarter core symmetry).
Loss coefficients from Table 7.2 (II)

POWER/FLOW (%/%)	ΔP CORE CONDOR	ΔP CORE PI	ΔP CORE PI / ΔP CORE CONDOR	HOT ASSEMBLY CHARACTERISTICS: W PI	W CONDOR	X PI	X CONDOR
88.0/72.2	[						
75.1/86.7							
95.8/95.2							
97.2/93.7							
99.6/90.8							
99.5/83.6							(a,c)
94.5/88.6							
76.3/67.4							
24.8/27.4							
99.7/99.7							
97.1/90.7							
50.4/44.7							]+

ΔP = Pressure drop, PSI
W = Assembly flow rate, 10^5 Lb/Hr
X = Assembly outlet quality, fraction
2120F:6

8.0 CONCLUSIONS

A general description is given of the CONDOR code. The CONDOR methodology is discussed, including the conservation equations, the void models and the pressure drop correlations. Qualification of the code is made using analytic solutions. Code predictions are compared with plant operating data. These discussions and predictions show that the CONDOR code is suitable for the design and analysis of BWR cores.

9.0 REFERENCES

1. E. Schmidt, "Properties of water and steam in SI-units," Springer-Verlag, Berlin, 1969.

2. A. J. Harris, L. T. Mayhue, C. M. Mildrum, "A Description of the Nuclear Design and Analysis Programs for Boiling Water Reactors," WCAP 10106, June 1982.

3. R. W. Dittus, L. M. K. Boelter, Univ. Calif. Publs. Engng. 2, p.443, 1930.

4. "TRAC-PIA, An advanced best estimate computer program for PWR LOCA analysis," NUREG/CR-0665, LA-7777-MS, May 1979, pp. 56-57.

5. R. P. Roy and S. Ho, "Influence of transverse intraphase velocity profile and phase fraction distributions on the character of two phase flow equations," Intl. J. Heat Mass Transfer, Vol, 23, pp. 1162-67, 1981.

6. S. Levy, "Forced convection subcooled boiling: Prediction of vapor volumetric fraction," GEAP-5157, April 1966.

7. N. Zuber et al, "Steady state and transient void fraction in two phase flow systems," Final report. Vol. I GEAP-5417 January 1967.

8. R. T. Lahey and F. J. Moody, "The Thermal Hydraulics of a Boiling Water Reactor", Chapter 5, ANS 1977.

9. C. J. Baroczy, "A systematic correlation for two-phase pressure drop," Heat Transfer Conf. (Los Angeles), Chem. Eng. Progr. Symp. Series No 64, Vol 62, 1966

10. A. S. F. Ansari, "Methods for the Analysis of Boiling Water Reactors Steady State Core Flow Distribution Code (FIBWR)," Yankee Atomic Electric Co., YAEC 1234, 12/31/80.

11. "Core Design and Operating Data for Cycle 1 of Hatch 1," EPRI-NP-562, Jan. 1979.

12. "Core Design and Operating Data for Cycles 1 and 2 of Peach Bottom 2", EPRI-NP-563, June 1978.

13. D. Chisholm, "Pressure Gradients due to Friction during the Flow of Evaporating Two-phase Mixtures in Smooth Tubes and Channels," Intl. J. Heat Mass Transfer, Vol. 16 p 347-358, 1973.

APPENDIX A LIST OF SYMBOLS

A_{X-S}	m^2	conventional flow area
Co	-	concentration parameter taking into account the flow distribution across the duct
cp_f	J/kg ^oC	specific heat of liquid
cp_v	J/kg ^oc	specific heat of steam
CPR	-	critical power ratio
D_e	m	hydraulic diameter
D_{film}	m	thickness of liquid film in annular flow
D_e	m	hydraulic diameter, fuel assembly
f	-	single phase friction factor
G	kg/m^2 s	mass flux
g	m/s^2	acceleration due to gravity
H_{sub}	J/kg	inlet subcooling
HF	J/kg	coolant enthalpy
H_f	J/kg	enthalpy of saturated liquid
H_{fg}	J/kg	enthalpy difference between saturated steam and water
h	W/m^2 ^oC	heat transfer coefficient
h_{BP}	W/m^2 ^oC	heat transfer coefficient between active and bypass flows
K	-	single phase local (form) loss coefficient
K1, K2, K3		constants in Levy's model
K_f	W/m ^oC	conductivity of water
K_{BOX}	W/m ^oC	conductivity of channel wall
K_{BP}	W/M^2 ^oC	heat transfer coefficient between active and bypass flows
L_H	m	heated length
P	N/m^2	pressure
P_S	N/m^2	saturation pressure as function of temperature
Pr	-	Prandtl number of water

P_H	m	heated perimeter
QA	W/m^2	local heat flux
Re	-	Reynolds number
S_{BOX}	m	thickness of box wall
T	^oC	temperature
T_B	^oC	bulk fluid temperature
T_w	^oC	temperature at the wall
V_{gi}	m/s	weighted mean drift velocity of vapor
W	kg/s	flow rate
W_f	m/s	liquid velocity at saturation temperature
X_e	%w	equilibrium quality
X_a	%w	actual steam quality (flow quality)
YBE	-	nondimensional distance to the tip of vapor bubble
Z_o	-	point of incipient vapor formation
Z	m	axial distance
α	%V	void fraction
ΔZ		axial node length
ΔP	N/m^2	pressure difference or pressure drop acc = acceleration el = elevation f = friction,
ΔT	^oC	temperature difference
ϕ^2	-	Two phase friction multiplier
ϕ^2_A	-	Acceleration multiplier
ϕ^2_{loc}	-	Two phase form loss multiplier
μ	kg/m·s	dynamic viscosity at saturation temperature
μ_f	kg/m·s	dynamic viscosity of saturated liquid

2120F:6/831209

APPENDIX A LIST OF SYMBOLS (CONTINUED)

μ_g	kg/m·s	dynamic viscosity of saturated steam
ρ_f	kg/m^3	density of saturated liquid
ρ_g	kg/m^3	density of saturated steam
$\Delta\rho$	kg/m^3	$\rho_f - \rho_g$
σ	N/m	surface tension

Subscripts

BOX	fuel channel
d	departure point
f	liquid
g	vapor
m	average
max	maximum
min	minimum
W	at the wall

RESPONSE TO

REQUEST NUMBER 1 FOR ADDITIONAL INFORMATION ON WCAP-10107

Question 1. In the calculation of acceleration pressure drop (page 3-2), only the irreversible ΔP due to the boiling process (voiding) is considered. The reversible ΔP due to area changes is not included. Explain the reason.

Response:

The reversible pressure drop due to flow area changes is not included in the CONDOR total core pressure drop calculation because the total pressure drop due to this between core inlet and outlet is zero. This is due to the flow area of the core inlet being equal to the flow area of the core outlet. This is demonstrated in the following:

The reversible pressure drop due to flow area changes can be expressed as

a) For single-phase flow:

$$\Delta P_{ACC} = \left[1 - \left(\frac{A_{outlet}}{A_{inlet}}\right)^2\right] \frac{\dot{m}^2}{2 g_c \rho_f A^2_{outlet}} \qquad (1)$$

where:

A_{outlet} = outlet flow area

A_{inlet} = inlet flow area

$g_c = 32.17 \dfrac{lb_m - ft}{lb_f - s^2}$

$\dot{m}$ = mass flow rate

ρ_f = fluid density

b) For two-phase flow:

$$\Delta P_{ACC} = \left[1 - \left(\frac{A_{outlet}}{A_{inlet}}\right)^2\right] \frac{\dot{m}^2 \rho_H}{2 g_c \rho_{ke}^2 A_{outlet}^2} \quad (2)$$

where:

$$\frac{1}{\rho_H} = \frac{X}{\rho_g} + \frac{(1 - X)}{\rho_\ell}$$

$$\frac{1}{\rho_{Ke}^2} = \frac{X^3}{\rho_g^2 \alpha^2} + \frac{(1-X)^3}{\rho_\ell^2 (1-\alpha)^2}$$

α = void fraction at outlet

x = steam quality at outlet

ρ_g = saturated vapor density

ρ_ℓ = saturated liquid density

The flow areas of the BWR core inlet and outlet are the same. Therefore, the reversible pressure drop across the core due to the flow area changes is zero.

Question 2. Justify Equation (3.8) for the calculation of bypass flows. Explain the methods for obtaining the constants C_1, C_2, C_3, and C_4. (These constants should depend strongly on fuel assembly design.)

Response:

Figure 2.1 is a schematic of the bypass flow paths that can occur for a W QUAD+ or a GE fuel assembly. Path (1), the water cross flow path, occurs only for the W QUAD+ fuel assembly. Path (9), the channel-lower tie plate (finger spring) path, occurs only for the GE-type fuel assembly. The bypass flow for both the W QUAD+ and GE fuel assemblies can be analyzed with the CONDOR code.

There are three separate equations in CONDOR that are used to calculate the flow in the inlet region of each leakage path. These are:

$$W_1 = C_1 (P_1-P_4)^{1/2}$$

$$W_2 = C_2 (P_2-P_4)^{1/2} \qquad \text{or} \qquad C'_2 (P_2-P_5)^{1/2}$$

$$W_3 = C_3 + C_4 (P_3-P_4)^{C_5}$$

where W_i is the flow for each type of path

$P_1, \ldots, P_5$ are the pressures indicated in Figure 2.1

$C_1, \ldots, C_5$ are constants.

It is seen that these equations are equivalent to equation (3.8).

The coefficients $C_1, \ldots, C_5$ are strongly dependent upon the fuel assembly design. The coefficients for paths (1) and (8) for the W QUAD+ fuel assembly are being determined from hydraulic tests of this fuel assembly. The coefficients for paths (2) to (9) for the GE fuel assembly were obtained by using the fraction of flow to each path given in Reference 2.1 and adjusting

001517-1

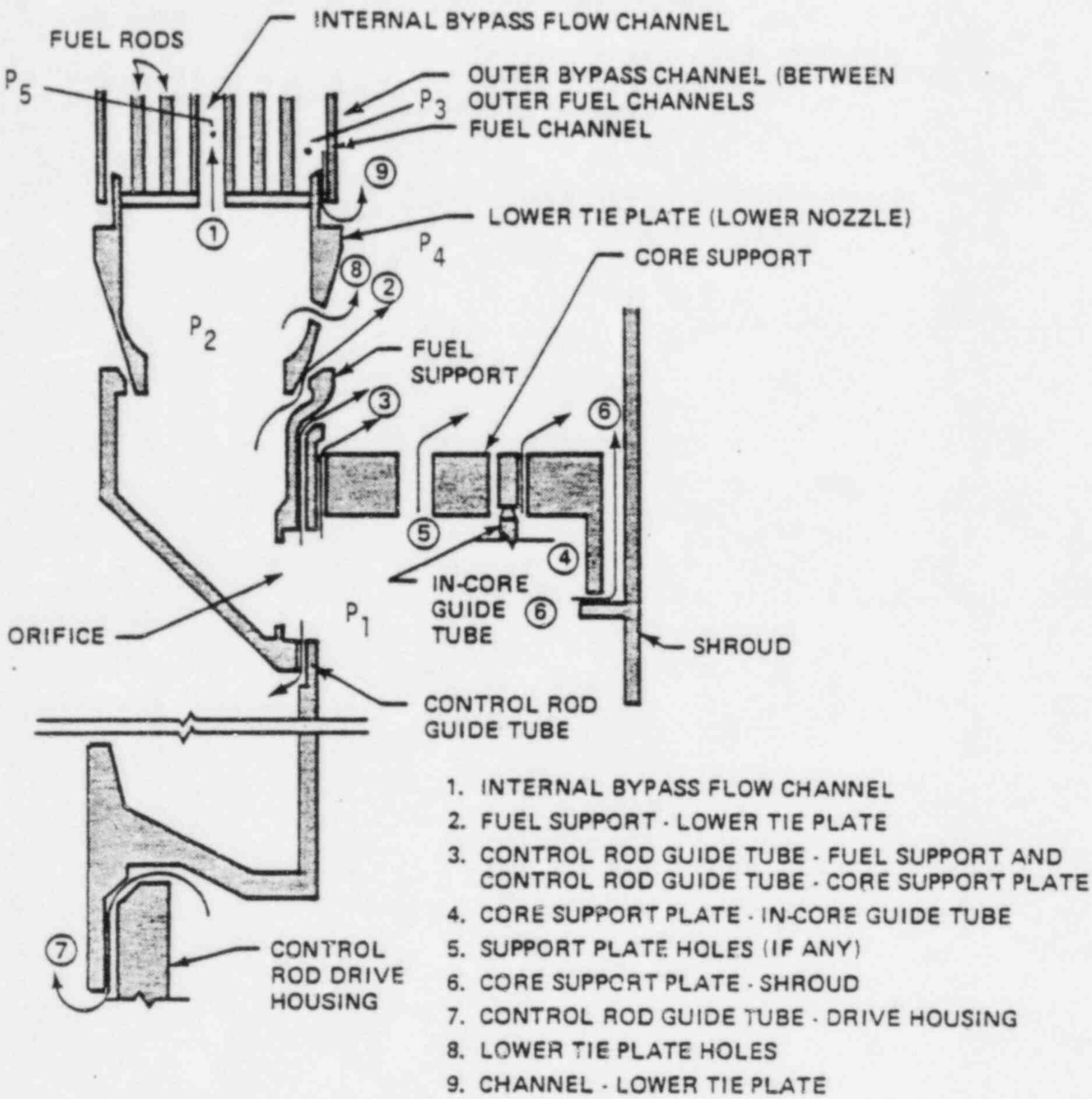

Figure 2.1. Schematic of Bypass Flow Paths

the coefficients $C_1, \ldots, C_5$ in the above equations until the proper fraction was obtained. Verification of this method was made by use of the equation for the finger spring path (path 9), given in Reference 2.2 and the equation for path (8) given in Reference 2.3. [ ] (a,c)

The equations listed above are for the inlet portion of each leakage path. CONDOR also calculates the pressure drop in the vertical portion of each leakage path. The equations to do this are those discussed in Section 3.2 of the topical, and thus include two-phase effects if there is any boiling in the bypass regions.

References

2.1 "BWR Fuel Channel Mechanical Design and Deflections," NEDO-21354, September, 1976.

2.2 A. A. Ansari, et. al., "FIBWR: A Steady-State Core Flow Distribution Code for Boiling Water Reactors Code Verification and Qualification Report," EPRI-NP-1923.

2.3 "Browns Ferry Nuclear Plant Units 1 and 2 SAR for Plant Modifications to Eliminate Significant In-Core Vibrations," NEDO-21091, November, 1975, Chapter 4.

Question 3. Item 6 on page 3-7 talks about the thermal-margin calculations, but no details are given. Please provide the actual methods used in the code for this calculation (e.g., correlations used).

Response:

Tests are being conducted to obtain critical power data for the <u>W</u> QUAD+ fuel assembly. The methodology to use these tests to calculate thermal margins is being developed. A separate topical on this will be submitted next year.

Question 4. Provide the sources for the data on 36 and 64 rod bundle tests as mentioned on pages 4-5.

Response:

The void-quality model used in the CONDOR code was developed using two sets of experiments on 36 rod bundles. The first set consisted of data from a 36 rod Marviken full scale test assembly (Test FT-36B) and the second set consisted of data from a 36 rod BWR type cluster (6x6 square array) (Test OF36). Both of these tests were conducted in the FRIGG BWR program in Sweden.

The void-quality model was later compared to three other sets of void measurements. The first was from a full scale BHWR 36 rod cluster (Test FT-36C). The second was from a full scale simulation of an Oskarshamn-1 (Asea-Atom) fuel assembly consisting of 64 rods in an 8x8 rectangular array using a radially symmetric power distribution (Test OF-64). The third test again used a full scale simulation of an Oskarshamn I fuel assembly consisting of 64 rods, this time using a radially skewed power distribution (Test OF-64b). These last three tests were also from the FRIGG BWR program.

Question 5. The CONDOR code has been benchmarked against two analytical solutions. These comparisons provide a check on the accuracy of the numerical and noding schemes. The benchmark did not provide separate-effects comparisons, namely the subcooled boiling model and the void-quality model. These models predict local voids. Their accuracy will affect the axial power distribution calculation in the neutronic and thermal-hydraulic iterations. Benchmark against FRIGG data (1) on subcooled boiling and void-quality relations should be made and the results should be submitted for review.

Response:

The FRIGG data referred to in Reference 1 (5.1) contains data that is part of the data base of the CONDOR void model (Test FT-36B). As discussed in the response to question 4, the CONDOR data base contains much more FRIGG data than that given in Reference 1. The results of the prediction of this data with the CONDOR void model were shown in Table 4.1 of the topical.

Reference:

5.1 Nylund, O., et. al., "Hydrodynamics and Heat Transfer Measurements on a Full Scale Simulated 36-Rod Marviken Fuel Element." ASEA-ATOM FRIGG Loop, R4-494/RTL-1154.

Question 6. The Baroczy correlation used in the CONDOR code is modified based on pressure drop data from 64-rod bundle tests. Provide the source of these data and the procedures used for the modification. A check on the correlation as given in the report showed that it underpredicts the two-phase multiplier, ϕ^2, at low qualities at $G = 1356\ kg/m^2s$ ($1 \times 10^6\ lb/hr\text{-}ft^2$) from the curves given by Baroczy (2) (a factor of 2 lower at $x = 0.02$).

Response:

The Baroczy method was used only as a starting point basis to develop the two-phase multiplier used in the CONDOR code. The Chisholm (6.1) correlation was used to approximate the Baroczy method. The exponents in the basic Chisholm correlation and in the property index expression were left unchanged since these constants are based on a theoretical model for two-phase friction. The rest of the correlation was modified and subjected to a least-square fitting procedure against the data base to give the correlation presented in the CONDOR topical.

The data base consisted of two-phase pressure drop data taken from full scale 64 rod bundles in the FRIGG loop test facility over a range of BWR conditions. This data base covered qualities up to around 40%. Above that region, the Baroczy correlation was selected to support ext polation up to single phase gas flow.

Since the Baroczy correlation was based on single tube data, one would expect differences when compared to full scale rod bundle data. At a quality x = .02, p = 1000 psi, and G = 1220 kg/m^2s (.9 x 10^6 $lb/hr\ ft^2$), the CONDOR two-phase multiplier $\phi^2 = 1.86$ is in good agreement with values of $\phi^2 = 1.8$ obtained by Isbin, et. al.(6.2) based on their measurements of steam-water flow at these conditions.

Referrences:

6.1 D. Chisholm, "Pressure Gradients due to Friction during the Flow of Evaporating Two-Phase Mixtures in Smooth Tubes and Channels," Intl. J. Heat Mass Transfer, Vol. 16, p. 347-358, 1973.

6.2 H. S. Isbin, et. al., "Two-phase Steam-Water Pressure Drops," Nucl. Engin. Pt. VI, Chem. Eng. Symp. Series No. 23, 55, 75-84 (1959).

Question 7. The mass flux range as stated on page 5-2 for the Baroczy correlation, 1 to 300 kg/m^2s, is not correct. The original Baroczy correlation covers a range of 339 to 4068 kg/m^2s. Explain the discrepancies.

Response:

This is a misprint. The range for the correlation is from 1 to 3000 kg/m^2s. As explained in the response to question 6, the data base was taken from full scale 64 rod bundles from the FRIGG test series for qualities up to around 40%. The Baroczy correlation was selected to support extrapolation to higher qualities.

Question 8. Explain how the water tubes are modeled. Describe geometric and hydrodynamic modeling.

Response:

The water tubes in a GE fuel assembly have not yet been explictly modelled with the CONDOR code. However, they can be easily modelled with the existing bypass flow and heat transfer equations described in Section 3.4. The inlet and exit losses for these tubes are given in Reference 8.1. The W QUAD+ fuel assembly does not have water tubes.

Reference:

8.1 A. A. Ansari, et. al., "FIBWR: A Steady State Core Flow Distribution Code for Boiling Water Reactor Code Verification and Qualification Report," EPRI-NP-1923.

Question 9. Describe how the CONDOR code is coupled with other codes for calculation of power distributions, MCPR, etc. (e.g., neutronics and systems codes) and justify the accuracy of its use for calculation of power distribution and MCPR.

Response:

The description of the coupling of the CONDOR code with the neutronics codes POLCA and PHOENIX is contained in the topical report concerning nuclear design and analysis submitted to the NRC.[9.1] The accuracy of these combined codes is justified if accurate power distributions are calculated by these combined codes. This will be discussed in a topical to be submitted in early 1984.

Reference:

9.1 A. J. Harris, L. T. Mayhue, C. M. Mildrum, "A Description of the Nuclear Design and Analysis Programs for Boiling Water Reactors," WCAP 10106, June 1982.

Question 10. The P1 outputs were used by Westinghouse to benchmark CONDOR calculations on core pressure drop, flow and quality distributions. Provide the detailed calculational procedure used by the P1 output of the process computer in [ ]† (a,c)

It is understood that the plant computer takes reactor boundary conditions such as total core flow, inlet subcooling and system pressure, and iterates on channel flows to obtain the final core flow and enthalpy distributions, similar to the scheme described in the CONDOR document. It raises a question about the usefulness of this benchmarking.

Response:

The detailed calculational procedure used by the [ ]† process computer to obtain the P1 output used to benchmark the CONDOR calculations is GE proprietary and thus unavailable to W. (a,c)

The benchmarking is useful from the following viewpoint. CONDOR will be used to obtain the flow and enthalpy distribution among the fuel assemblies in the core. The CONDOR predictions given in the topical show that the hot channel flows and enthalpies were accurately predicted using either values of loss coefficients obtained from open literature reports or loss coefficients based on [ ]† Since the process computer is used to monitor the fuel operating limits, this implies that CONDOR can reliably be used to calculate the operating margin to these limits. CONDOR will be used in the calculation of the fuel operating limits for a mixed vendor core or an all W core. The loss coefficients to be used in CONDOR for such a calculation will be obtained from measurements by W using the same test facility as was used for W test of P8x8R fuel assembly. (a,c)

Questions on nomenclature and/or misprints.

Response:

All the typographical errors and misprints are corrected and the revised copy is attached.